

Coupling Effects in Dense Arrays of 3D Optical Metamaterials

D. Bruce Burckel^{*a}, Bryan M. Adomanis^b, Salvatore Campione^a, and Michael B. Sinclair^a

^aSandia National Laboratories, Albuquerque, NM USA 87185; ^bAir Force Research Laboratory, 3005 Hobson Way, Wright Patterson AFB, OH USA 45433,

ABSTRACT

Three-dimensional (3D) metafilms composed of periodic arrays containing single and multiple micrometer-scale vertical split ring resonators per unit cell were fabricated using membrane projection lithography. In contrast to planar and stacked planar structures such as cut wire pairs and fishnet structures, these 3D metafilms have a thickness $t \sim \square \square d/4$, allowing for classical thin film effects in the long wavelength limit. The infrared specular far-field scattering response was measured for metafilms containing one and two resonators per unit cell, and compared to numerical simulations. Excellent agreement in the frequency region below the onset of diffractive scattering was obtained. The metafilms demonstrate strong bi-anisotropic polarization dependence. Further, we show that for 3D metafilms, just as in solids, complex unit cells with multiple atoms (inclusions) per unit cell possess a richer set of excitation mechanisms. The highlight of these new coupling mechanisms is the excitation of the 3D analog to the 2D cut-wire-pair magnetic response.

Keywords: Metamaterials, 3-Dimensional, Coupling

1. INTRODUCTION

In the seminal paper on metamaterials [1], the split ring resonator (SRR) was advanced as a possible meta-atom which could provide a magnetic behavior in a spectra region where magnetic activity is absent in natural materials. In the microwave regime, SRRs can be created with multiple concentric split rings and with separations and gaps that are significantly smaller than the operational wavelength of the material. Scaling this structure into the optical regime provides several complications which render the SRR less useful. Fabrication of small scale SRRs with dimensions of the order of micrometers typically requires the use of single split rings [2,3], which necessarily allow for bianisotropic excitation, where both the magnetic field as well as the electric field of an incident plane wave can excite the fundamental resonance of the SRR [4-6]. Furthermore, while the SRR functions as a source for artificial magnetism at microwave frequencies, the ability of SRRs to provide negative permeability at higher frequencies is limited by electron kinetic energy [7] and other deleterious effects which cause the magnetic polarizability to saturate with increasing frequency.

These difficulties associated with SRRs have led to the emergence of alternative meta-atoms for achieving magnetic behavior in the optical regime [8]. Both the fishnet structure [9-11] and cut-wire pairs [12-13], two stacked planar structures, have demonstrated more robust magnetic behaviors at optical frequencies due to their unique excitation mechanism. In both of these stacked planar cases, asymmetric current flow in the parallel metal traces creates a virtual current loop and hence magnetic response. In both cases, however, the excitation of the magnetic resonance is actually a bianisotropic response, where both the magnetic and electric field are capable of driving the resonance associated with the magnetic polarizability moment [14].

The vast majority of nano/microfabrication approaches are only capable of creating 2-dimensional structures, which are limited in the manner in which they can achieve coupling to incident electromagnetic fields as well as mutual coupling between neighboring inclusions. Three-dimensional fabrication approaches for structures with length scales in the micrometer and sub-micrometer regime are much less common than their two-dimensional brethren. Layer-by-layer approaches [15] can be used to create stacked versions of planar inclusions. Direct laser write [16] and nano-origami [17, 18] approaches can be used to create fully three dimensional structures; however the structures that can be realized by these fabrication approaches may be limited in either form factor or areal packing density of inclusions. Recently Tsai et.

^{*}dbburck@sandia.gov;

al. [19] have demonstrated vertical split ring resonators (VSRRs) with their gaps oriented on the top of the SRR, fabricated by a two-write e-beam fabrication sequence, and measured enhancement of the magnetic field. While this two-write e-beam approach is capable of fabricating high resolution VSRRs resonant in the optical regime, it would be difficult to create VSRRs with other orientations, such as having the gap to the side.

The recent emergence of planar metasurfaces [20-22], where the thickness t is significantly thinner than the design wavelength λ_d (i.e. $t \ll \lambda_d$), is further evidence of the potential power of structured materials. Despite this success, planar configurations are limited in the possible spatial orientations, packing density and interaction mechanisms with incident light. Combining the powerful apparatus and design insight of planar metasurfaces with more conventional 3D thin film

In the original vision of metamaterials, metallic structures significantly smaller than $\sim d$ impart electric and magnetic polarizability at a spatial granularity which precludes exchange of momentum with the lattice, and the emergence of diffractive scattering. In practice, most structured materials deviate from this point-approximation, with larger scale resonant structures such as split ring resonators (SRRs) arranged on a lattice with sufficiently small characteristic lattice momentum that diffraction from the lattice must frequently be considered. In addition, the inclusions cannot be treated as homogeneous atoms and typically possess a spectrum of individual normal modes, as well as mutual interactions with neighboring inclusions, complicating the simple polarizability notion.

2. RESULTS AND DISCUSSION

2.1 Metafilm fabrication:

The metafilms were created using membrane projection lithography [23-25]. The fabrication was carried out on a 150 mm silicon CMOS fabrication line with 248 nm optical scanner. Square cavities ($2 \mu\text{m} \times 2 \mu\text{m}$) in a $2.3 \mu\text{m}$ period square array ($1 \text{ cm} \times 1 \text{ cm}$ lateral dimensions for the entire array) were etched into silicon wafers to a depth of $3 \mu\text{m}$ using a photoresist/silicon nitride etch mask (**Fig. 1(a)**). The wafer was oxidized to thin the silicon walls to $\sim 100 \text{ nm}$. The cavities were backfilled with polysilicon and polished back to planarize, stopping on the nitride. 100 nm of aluminum nitride was deposited and patterned with a SRR with as-drawn mask dimensions given in **Fig. 1(b)**. A chemical downstream etch was used to remove the polysilicon backfill material and a hydrofluoric acid etch removed the wall-thinning oxide. The SRRs were deposited via non-rotated oblique e-beam evaporation (**Fig. 1(c)**), consisting of a Chromium/Gold stack (10 nm/50 nm) at 2 \AA/s . Multi-SRR-basis films were created by performing successive evaporation through the membrane with a substrate rotation (either 90° or 180°) between depositions. The metal-coated AlN was removed via SC1 clean ($\text{pH} \sim 10$ - $\text{H}_2\text{O}:\text{NH}_4\text{OH}: \text{H}_2\text{O}_2$, 5:1:1 at 70°C), yielding the metafilm array.

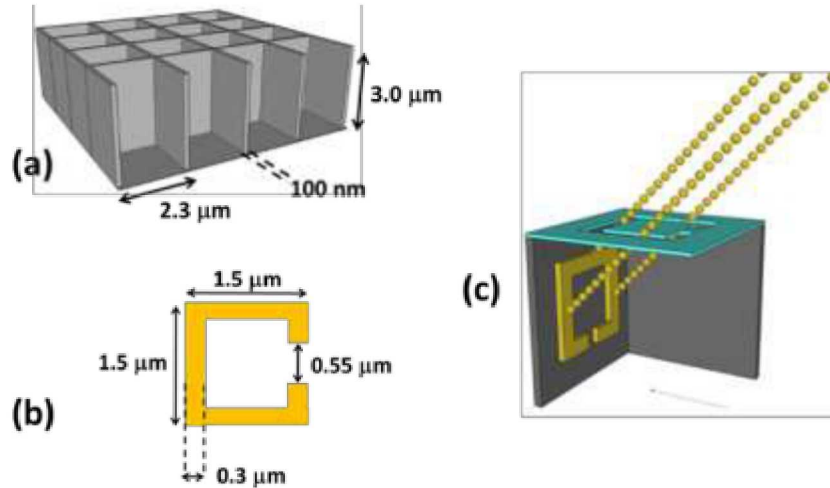


Fig. 1 (a) Physical dimensions of the unit cell; (b) Physical dimensions of the “as-drawn” split ring resonators; (c) Schematic of the angled evaporation process in membrane projection lithography.

Fig. 2 shows an SEM image of a 5-SRR-basis unit cell, where 5 depositions of the SRR pattern (4 on the walls, and one on the floor) were performed. Depending on the e-beam imaging conditions, the thin silicon walls can allow visibility of the SRRs on the back sides of the unit cell walls. This close proximity of the SRRs in the matrix allows for tight coupling between next-nearest-neighbor unit cells.

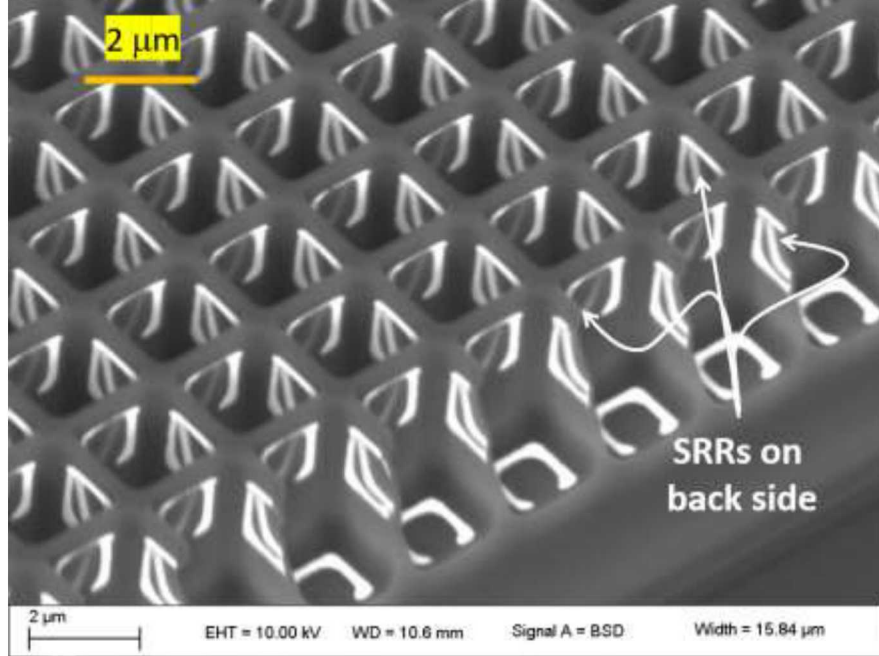


Fig. 2 SEM image of a 5-SRR basis unit cell demonstrating the proximity of SRRs in neighboring unit cells. This tight separation is crucial for the coupling between back-to-back SRRs.

2.2 Optical measurements

For the fabrication of the measured devices, two evaporation of the SRR pattern were performed with a 180° rotation between evaporation so that the resulting unit cells had one gap-up and one gap-down SRR positioned on opposing walls. The thin unit cell walls enable coupling between the SRRs from the adjacent cells. Vertically oriented (both single and multiple ring) SRRs have coupling mechanisms that their planar brethren do not [26-28]. We show here that these back-to-back SRRs possess yet another coupling mechanism which has previously seen little discussion. The far-field scattered light was examined using a hemispherical directional reflectometer (HDR) connected to a Nicolet FTIR. At normal incidence, low frequency light lacks sufficient momentum to resolve and diffract from the periodic array of boxes. Above this frequency, diffracted orders exist, first in the high index substrate and finally in the low index air above the array (indicated by the grey region to the right of 75THz in the plots in Fig. 3). In addition to the measured data, the structures were modeled with commercial rigorous coupled wave analysis (RCWA) software, retaining the first 19 modes.

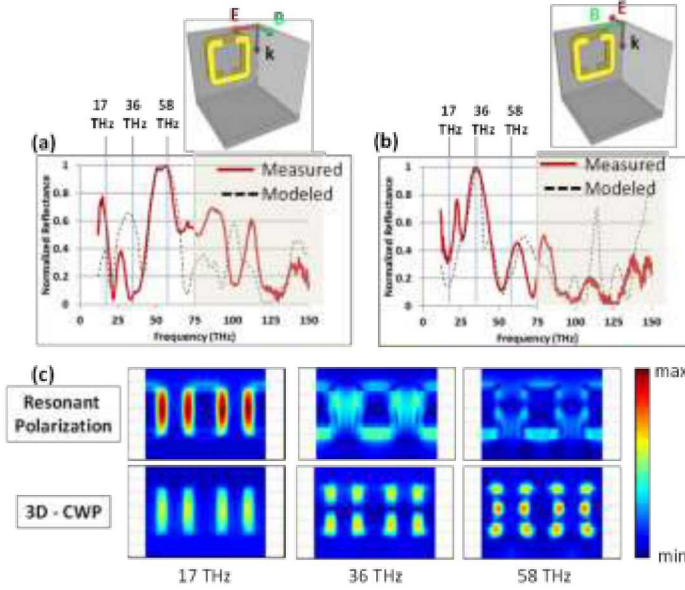


Fig. 3(a) Measured scattering response for resonant polarization; (b) Measured scattering response for the 3D analog of the cut-wire pair; (c) Field plots through center of the wall containing the back-to-back SRRs for both polarizations.

Consider the 2-SRR-basis unit cell in the upper insets of **Fig. 3**. In this case the cubic unit cell contains a gap-up SRR and a gap-down SRR located on opposite interior faces of the cavity. In a periodic array, this arrangement results in back-to-back SRRs in next-nearest-neighbor unit cells (one gap-up, one gap-down) separated by the thickness of the cavity wall. While intra-cell coupling is possible across the width of the cavity, the proximity of the SRRs in next-nearest-neighbor unit cells enables strong inter-cell coupling. In **Fig. 3** (a), the polarization is chosen so the E-field is in the X-Z plane containing the SRRs, the resonant polarization for both the gap-up and gap-down SRRs. In **Fig. 3** (b), the orthogonal polarization, corresponding to the transparent polarization for a single SRRs is shown. The B-field parallel to the closely spaced back-to-back SRRs results in an induced current on the opposite arms of the SRRs.

The field profiles in **Fig. 3** (c) show the magnitude of the magnetic field in the center of the cavity wall between the two SRRs for both the resonant and transparent polarizations at three different frequencies. The field plots of the 3D-CWP mode shows a clear progression in node number with increasing frequency, while the driven field plots are more complicated. The highest magnitude of the magnetic field occurs for the resonant polarization at 17 THz, however the 3D-CWP resonance is a significant fraction of this maximum value. At higher frequencies, the strength of the magnetic field in the gap for the 3D-CWP resonance surpasses that of the resonant polarization.

2.3 FDTD simulations

Fig. 4 contains a finite difference time domain (FDTD) simulation (performed using Lumerical FDTD) of the absorption spectra (un-scaled) for both gap-up and the back-to-back gap-up/gap-down SRRs under resonant and transparent polarizations. For visualization purposes, only the SRRs are shown in the polarization insets; however the simulation modeled the entire unit cell with dispersive optical constants. The raw curves are shifted vertically by 0.4 for clarity (see red arrow). Coupling to the second SRR is obvious for both polarizations. In the resonant polarization, there is an increase in the relative strengths of the peaks, and the introduction of asymmetric lineshapes in some peaks. In the orthogonal polarization the emergence of the 3D-CWP resonance (dashed black circles), is clearly observed.

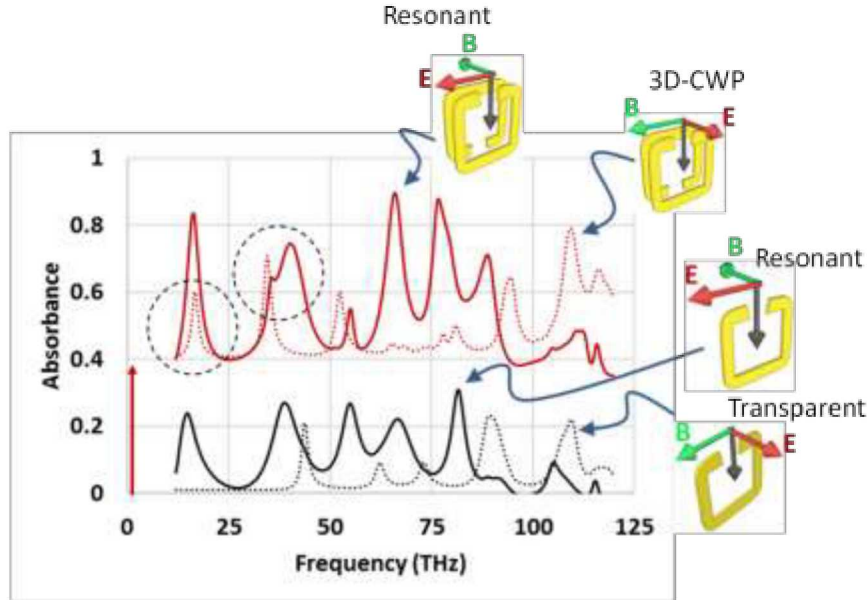


Fig. 4 Absorbance versus frequency of the 3D-CWP.

3. CONCLUSION

Here we have shown measured and modeled reflection data demonstrating several unique properties of 3D metafilms, and how the optical behavior of the film can be modified by using multi-SRR basis unit cells. For 2-SRR-basis unit cells with inclusions on opposite faces, the film can respond to both incident linear polarizations in either a directly driven resonance or through the excitation of the 3D-CWP resonance. These 2-SRR-basis films possess excitation mechanisms and polarization behaviors which cannot be attained in planar, or stacked planar configurations, and hint at even richer electromagnetic behaviors for metafilms composed of 3-SRR and higher bases. In this way we have gained multiple degrees of freedom to manipulate the effective behavior of 3D metafilms; one may also think of using other shapes other than SRRs, and this will further provide ways to manipulate the light-matter interaction in these 3D metafilms.

ACKNOWLEDGEMENTS

This paper describes objective technical results and analysis. Any subjective views or opinions that might be expressed in the paper do not necessarily represent the views of the U.S. Department of Energy or the United States Government. This work was performed, in part, at the Center for Integrated Nanotechnologies, an Office of Science User Facility operated for the U.S. Department of Energy (DOE) Office of Science. Supported by the Laboratory Directed Research and Development program at Sandia National Laboratories, a multi-mission laboratory managed and operated by National Technology and Engineering Solutions of Sandia, LLC., a wholly owned subsidiary of Honeywell International, Inc., for the U.S. Department of Energy's National Nuclear Security Administration under contract DE-NA-0003525. Partially supported by the Defense Advanced Research Projects Agency Defense Sciences Office (DSO) Program: DARPA/DSO EXTREME; Agreement No. HR0011726711.

REFERENCES

[1] Pendry, J.B., Holden, A. J., Robbins, D. J., and Stewart, W. J., "Magnetism from conductors and enhanced nonlinear phenomena," *IEEE Trans. On Microwave Theory and Techniques*, 47, no 11, 2075-2084, (1999).

[2] Katsarakis, N., Konstantinidis, G., Kostopoulos, A., Penciu, R. S., Gundogdu, T. F., Kafaesaki, M., Economou, E. N., Koschny Th. and Soukoulis, C. M., "Magnetic response of split-ring resonators in the far-infrared frequency regime," *Optics Letters*, 30(11), 1348-1350 (2005).

[3] Rockstuhl,C, Lederer,F., Etrich,C, Zentgraf,T, Kuhl, J, and Giessen,H., "On the reinterpretation of resonances in split-ring-resonators at normal incidence," *Optics Express*, 14, 8827-8836 (2006).

[4] Katsarakis, N., Koschny, T., Kafesaki, M., Economou, E. N. and Soukoulis, C. M., "Electric coupling to the magnetic resonance of split ring resonators," *Applied Physics Letters*, 84, 2943 (2004).

[5] Marques,R., Medina,F., and El-Idrissi,R.R., "Role of bianisotropy in negative permeability and left-handed metamaterials," *Physical Review B*, 65, 144440 (2002).

[6] Feth,N., Konig, M. , Husnik, M. , Stannigel, K. , Niegemann, J. , Busch, K. , Wegener, M. , and Linden, S. "Electromagnetic interaction of split-ring resonators: The role of separation and relative orientation," *Opt. Exp.*, 18(7), 6545-6554 (2010).

[7] Zhou, J., Koschny, Th., Kafesaki, M., Economou, E. N., Pendry, J. B. and Soukoulis, C. M., "Saturation of the magnetic response of split-ring resonators at optical frequencies," *Physical Review Letters*, 95, 223902 (2005).

[8] Monticone, F. and Alu, A. , "The quest for optical magnetism: from split-ring resonators to plasmonic nanoparticles and nanoclusters," *Journal of Materials Chemistry C*, 2, 9059-9072 (2014).

[9] Zhang, S. , Fan, W. Panoiu, N. C. , Malloy, K. J. , Osgood, R. M. and Brueck, S. R. J. , "Experimental demonstration of near-infrared negative-index metamaterials," *Physical Review Letters*, 95, 137404 (2005).

[10] Penciu, R. S. , Kafesaki, M. , Koschny, Th. , Economou, E. N. , and Soukoulis, C. M. , "Magnetic response of nanoscale left-handed metamaterials," *Physical Review B*, 81, 235111 (2010).

[11] Xiao, S. , Drachev, V. P., Kildishev, A. V. Ni, X. , Chettiar, U. K., Yuan, H.K and Shalaev, V. M. , "Loss-free and active optical negative index metamaterials," *Nature*, 466, 735-738 (2010).

[12] Dolling, G., Enkrich, C. , Wegener, M. , Zhou, J. F. ,Soukoulis, C.M. and Linden, S., "Cut-wire pairs and plate pairs as magnetic atoms for optical metamaterials," *Optics Letters*, 30(23), 3198-3200 (2005).

[13] Shalaev, V. M. , Cai, W. , Chettiar, U. K. , Yuan, H.-K. , Sarychev, A. K., Drachev, V. P. and Kildishev, A. V. , "Negative index of refraction in optical metamaterials," *Optics Letters*, 30(24), 3356-3358 (2005).

[14] Burckel, D. B., Adomanis, B. M., Sinclair, M. B. and Campione, S., "Three dimensional cut-wire pair behavior and controllable bianisotropic response in vertically oriented meta-atoms," *Optics Express*, 25 (25), 32198-32205 (2017).

[15] Liu N.; Liu H.; Zhu S.; Giessen H. *Stereometamaterials*. *Nat. Photon.*, 3, 157-162 (2009).

[16] Gansel J.K.; Thiel M.; Rill M.S.; Decker M.; Bade K.; Saile V.; von Freymann G.; Linden S.; Wegener M. *Gold helix photonic metamaterial as broadband circular polarizer*. *Science*, 325, 1513-1515 (2009).

[17] Cho J.H.; Keung M.D.; Verellen N.; Lagae L.; Moschalkov V.V.; Van Dorpe P.; Gracias D.H. *Nanoscale origami for 3D optics*. *Small*, 7, 1943-1948 (2011).

[18] Joung D.; Agarwal K.; Park H.R.; Liu C.; Oh S.H.; Cho J.H. *Self-assembled multifunctional 3D microdevices*. *Adv. Elec. Mater.*, 2, doi: 10.1002/aelm.201500459 (2016).

[19] Chieh,P, Hsu, W.L., Chen, W.T., Huang, Y.W., Liao,C.Y., Liu, A. Q., Zheludev, N.I., Sun,G., and Tsai,D.P., "Plasmon coupling in vertical split-ring resonator metamolecules," *Scientific Reports*, 5:9726, DOI: 10.1038/srep09726 (2015).

[20] Ra'di,Y., Sounas D.L. and Alu,A, "Metagratings: Beyond the limits of graded metasurfaces for wave front control," *Phys. Rev. Lett.*, 119, 067404, (2017).

[21] Kildishev, A. V., Boltasseva, A., and Shalaev, V. M. "Planar photonics with metasurfaces," *Science*, 339, 1232009 (2013)

[22] Yu, N. and Capasso, F, "Flat optics with designer metasurfaces," *Nat. Mater.*, 13, pp. 139-150 (2014).

[23] Burckel, D. B, Wendt,J.R. Ten Eyck,G.A, Ginn,J.C., Ellis, A.R., Brener, I. and Sinclair,M.B. "Micrometer-scale cubic unit cell 3D metamaterial layers," *Adv. Mater.*, 22(44), 5053-5057 (2010).

[24] Burckel, D. B. , Resnick, P. J. , Finnegan, P. S. , Sinclair, M.B. and Davids, P. S. , "Micrometer-scale Fabrication of complex three-dimensional lattice+basis structures in silicon," *Opt. Mater. Expr.*, 5, 2231-2239 (2015).

[25] Burckel, D. B, Campione,S., Davids, P.S. and Sinclair, M.B., "Three dimensional metafilms with dual channel unit cells," *Applied Physics Letters*, 110, no 14, 143107 (2017).

[26] Marques,R. Mesa,F, Martel, J. and Medina,F., "Comparative analysis of edge- and broadside-coupled split ring resonators for metamaterial design – theory and experiments," *IEEE Transactions on Antennas and Propagation*, 51(10), 2572-2581 (2003).

- [27] Fan,K, Strikwerda,A.C., Tao,H. , Zhang,H., and Averitt, R.D., “Stand-up magnetic metamaterials at terahertz frequencies,” *Optics Express*, 19(13), 12619-12627 (2011).
- [28] Zeng,Y., Dineen, C., and Moloney, J.V.,“Magnetic dipole moments in single and coupled split-ring resonators,” *Physical Review B*, 81, 075116 (2010).